Nordic Hydrology, 31 (1), 2000, 57-72

Numerical Modelling of Circulation in Lake Sperillen, Norway

N. R. B. Olsen and D. K. Lysne

Norwegian University of Science and Technology,
N-7034 Trondheim, Norway

A three-dimensional numerical model was used to model water circulation and spatial variation of temperature in Lake Sperillen in Norway. A winter situation was simulated, with thermal stratification and ice cover. The numerical model solved the Navier-Stokes equations on a 3D unstructured non-orthogonal grid with hexahedral cells. The SIMPLE method was used for the pressure coupling and the k-ε model was used to model turbulence, with a modification for density stratification due to the vertical temperature profile. The results were compared with field measurements of the temperature in the lake, indicating the location of the water current. Reasonably good agreement was found.

Introduction

Lake Sperillen is located 60 km north of Oslo in Norway at 150 m above sea level. It is 20 km long, 1-2 km wide and has a maximum depth of 129 metres. In the winter, the ice thickness can be fairly great for several weeks, providing support for transport by the local population. After the construction of a hydropower plant discharging water into the lake in 1964, one of the local farmers complained that the ice thickness had decreased. The ice did not support a man on skis any more, on the west side of the lake. The statement prompted an investigation into the ice thickness, water temperature and hydrodynamics of the lake.

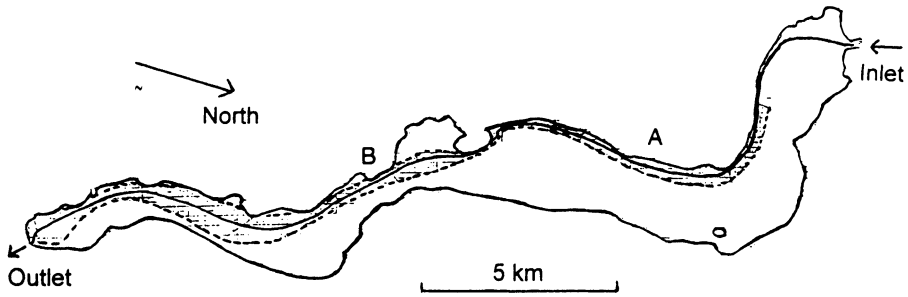

Fig. 1. Lake Sperillen seen from above, with the measured centreline and the horizontal location of the current (Friis 1969). The arrows show the point of inflow and outflow. The letters A and B denote sections where velocity measurements were taken.

The initial investigations started with measuring the ice thickness. Between January and March, the thickness was usually large enough to support transportation of people, enabling measurements to take place. The thickness was measured to 70-80 cm in March 1964 (Friis 1969), with a relatively uniform distribution in the lake, except for a slight decrease on the west side of the lake. In the two winters from 1968 to 1969, a number of temperature measurement campaigns were carried out in the lake (Friis 1969). Each time, measurements were taken in 12 cross-sections, with a number of vertical profiles in each section, less than 100 metres apart. The temperatures were measured at depths of 1, 2, 3, 4, 5, 7, 10, 15, 20, 25, 30, 40 and 50 metres. The profiles showed a classical winter lake stratification, with cold water of about 0.1°C close to the ice-covered surface and a temperature of about 3.8°C at the bottom of the lake. However, at the west side of the lake, close to the surface, there was an anomaly, as the temperature was higher and more uniform than in the rest of the cross-section. It was concluded that this was due to a short-circuiting of the lake by the inflow from a river entering from the northern side (Friis 1969). The outflow was at the south end of the lake. Fig. 1 shows the lake, with the measured centreline of the current from the winter of 1968. The measurements were repeated several times throughout the winter of 1969, and all measurements showed the same location of the current.

The location of the current was determined from the field data based on the vertical temperature gradient parameter, S, calculated from the following formula

$$S = \frac{T_{10}+T_7}{2} - \frac{T_5+T_4+T_3}{3} \qquad (1)$$

The index denotes the level (m) under the ice where the temperature, T, was measured. The value of S was below 0.3°C/m in the shaded area of Fig. 1. Outside the shaded area, the value was above 0.3°C/m, indicating a steeper gradient.

In 1975, Stigebrandt (1977) measured current velocities directly in two cross-sec-

tions of the lake. One day was used for each cross-section, and the measurements were not repeated. An ultrasonic current meter was used, with a sensitivity of a few mm/s. In cross-section A, the measured centre of the current corresponded well with Friis' measurements. However, Section B showed a more uniform velocity profile in the horizontal direction compared with Friis. This will be discussed later.

The purpose of the present study was to test a 3D numerical model and its ability to model processes in a lake, in particular the circulation. If the model worked well, it could be used to predict environmental impacts of changes in the water discharge flowing into the lake, or its temperature. Many lakes in Norway receive water from hydropower plants, and with new peaking regulations the water flow into the lakes will change. A general 3D numerical model could also be used for other environmental studies, for example pollution control.

Previously, numerical modelling has been used in several studies of lakes. Early work was carried out by Simons (1976), simulating wind-induced circulation in Lake Ontario. A three-dimensional finite difference method was used, with a constant eddy-viscosity model describing the turbulence. The eddy-viscosity was varied until the computational result agreed with the measurements. A model similar to Simons was used by Huttula *et. al.* (1996) to model wind induced currents in Lake Pyhaselka in Finland. Also, the concentrations of oxygen, phosphorus and phytoplankton were calculated, as waste water from a paper mill and a town were discharged into the lake. Rajar and Cetina (1997) used a similar approach model to calculate wind and current induced circulation and water quality in a lake.

Falconer *et. al.* (1991) modelled Esthwaite Water in the UK using the same approach. Esthwaite was relatively shallow, and density stratification was not taken into account. Good agreement was found with field measurements of water velocities, after calibration of a constant eddy-viscosity model. Two-dimensional models have also been used extensively for studies of lakes and reservoirs. A depth-averaged approach have most often been used, for example Olsen (1999a) calculating flushing of sediments from a hydropower reservoir. Also a width-averaged approach have been applied. Malm (1995) calculated circulation in a 2D width-averaged lake geometry using the SIMPLE method for pressure coupling and algebraic zero-equation turbulence models. The thermal bar was modelled, and the influence of shear stresses and density currents were investigated. The results showed many similarities with field observations.

Gbah *et. al.* (1998) used a Reynolds stress turbulence model to calculate the wind-induced water currents and temperature in a thermal bar for an idealised two-dimensional width-averaged case. The advantage of the sophisticated turbulence model was that the eddy-viscosity was calculated as a part of the flow field, and did not need to be specified by the user. The model could thereby be applied to new cases without calibration. Gbah *et. al* found good results for the thermal bar migration speed, compared with field data. A combination of an advanced turbulence model and a fully 3D calculation was also done by Olsen *et. al.* (1994). The k-ε turbulence

model was used solving the Navier-Stokes equations on a 3D grid of a hydropower reservoir. The reservoir was relatively shallow and there was no density stratification. The calculated water circulation compared well with field measurements without calibration of the turbulence model. The reservoir was in this case modelled with a structured quadrilateral grid. In the present study, an unstructured quadrilateral grid was used. The unstructured grid is more flexible for modelling complex geometries.

Guting and Hutter (1998) also used the k-ε turbulence model to calculate the vertical eddy-viscosity when modelling 3D circulation in a homogenous lake. A number of advantages were pointed out compared with more primitive turbulence models, for example a clear correspondence between the water velocity and the turbulence. Also the effect of inertial waves on the turbulence was modelled. Guting and Hutter obtained good correspondence with field measurements, including modelling of the Ekman spiral. However, the numerical model used a constant eddy-viscosity model in the horizontal directions. In the present study the k-ε model was used in all three directions. Also, the lake modelled in the present study was stratified, giving added complexity.

The Numerical Model

The numerical model calculated the water flow by solving the Reynolds averaged transient Navier-Stokes Equations

$$\frac{\partial U_i}{\partial t} + U_j \frac{\partial U_i}{\partial x_j} = \frac{1}{\rho} \frac{\partial}{\partial x_j} \left(-P \delta_{ij} - \rho \overline{u_i u_j} \right) \tag{2}$$

U is the averaged water velocity in a time step, t is the time, x is a space coordinate, ρ is the water density, P is the pressure, δ_{ij} is the Kronecker delta, which is 1 if $i=j$ and 0 otherwise. The fluctuating velocity in a time step when U is subtracted is denoted u. Eq. (2) was discretized using a control volume approach. An implicit method was used to discretize the transient left term on the left side of the equation. The second term on the left side of the equation is the convective term. Two upwind methods were used for this term: the Power-Law Scheme (POW) and the Second Order Upwind (SOU) method. The POW scheme has a first order accuracy, and the SOU scheme has second order accuracy.

The first term on the righthand side of Eq. (2) is the pressure term. The SIMPLE method was used to find the pressure. Patankar (1980) describes this method in more detail. The second term on the right side of the equation is the Reynolds stress term. The k-ε turbulence model was used in the present study. The eddy-viscosity concept was therefore used

$$-\overline{u_i u_j} = \nu_T \frac{\partial U_i}{\partial x_j} - \frac{2}{3} k \delta_{ij} \tag{3}$$

The eddy-viscosity is given as

$$v_T = c_\mu \frac{k^2}{\varepsilon} \tag{4}$$

k is turbulent kinetic energy, defined by

$$k \equiv \frac{1}{2} \overline{u_i u_i} \tag{5}$$

k was modelled as

$$\frac{\partial k}{\partial t} + U_j \left(\frac{\partial k}{\partial x_j} \right) = \frac{\partial}{\partial x_j} \left(\frac{v_T}{\sigma_k} \frac{\partial k}{\partial x_j} \right) + P_k - \varepsilon \tag{6}$$

P_k is given by

$$P_k \equiv v_t \frac{\partial U_i}{\partial x_j} \left(\frac{\partial U_j}{\partial x_i} + \frac{\partial U_i}{\partial x_j} \right) \tag{7}$$

ε was modelled as

$$\frac{\partial \varepsilon}{\partial t} + U_j \frac{\partial \varepsilon}{\partial x_j} = \frac{\partial}{\partial x_j} \left(\frac{v_T}{\sigma_\varepsilon} \frac{\partial \varepsilon}{\partial x_j} \right) + C_{\varepsilon 1} \frac{\varepsilon}{k} P_k - C_{\varepsilon 2} \frac{\varepsilon^2}{k} \tag{8}$$

In the above equations c_μ, σ_k, σ_e, C_{e1} and C_{e2} are different constants with values 0.09, 1.0, 1.3, 1.44 and 1.92 respectively. Note the eddy-viscosity is isotropic, and the same value is used in both the vertical and horizontal directions. The turbulence model is described in more detail by Rodi (1980).

The effect of temperature stratification on turbulence damping was taken into account by decreasing the turbulent eddy-viscosity, v_T, as a function of the water density gradients according to the following formula (Rodi 1980)

$$v_T = v_{T,0} \left(1 + \beta \left(-\frac{g}{\rho} \frac{(\partial \rho / \partial z)}{(\partial U / \partial z)^2} \right) \right)^\alpha \tag{9}$$

Here, g is the acceleration of gravity, z is the coordinate in the vertical direction, and α and β are constants. The default values are $\alpha = -0.5$ and $\beta = 10$ for the velocity equations, and $\alpha = -1.5$ and $\beta = 3.33$ for the other equations (Rodi 1980).

The temperature, T, was calculated by solving the convection-diffusion equation for heat transport

$$\frac{\partial T}{\partial t} + U_j \frac{\partial T}{\partial x_j} = \frac{1}{\rho} \frac{\partial}{\partial x_j} \left(\Gamma_T \frac{\partial T}{\partial x_j} \right) \tag{10}$$

The diffusion coefficient, Γ_T, was set equal to the eddy-viscosity taken from the k-ε model.

A formula for the water density as a function of the temperature was used to evaluate Eq. (9). The density gradients were taken into account as extra source terms in

the Navier-Stokes equations similar to a model using the hydrostatic pressure assumption, resulting in source terms only in the horizontal direction. The alternative, using the variable density in the vertical direction, lead to very large source terms and instabilities.

The Coriolis force was also included as an extra source term in the Navier-Stokes equations. A Coriolis parameter of 0.00013 was used. No-slip boundary conditions were used for all variables at the bed, sides and the ice. A zero-gradient boundary condition was used for the outflow. The values were specified on the inflow boundary. The temperature flux across the ice was modelled by including a source term in the heat equaton. The source term was based on a heat balance for the lake, from the measured temperatures in the lake and at the inlet and outlet.

The numerical models and discretization procedures are described in more detail by Patankar (1980) and Olsen (1999b).

Circulation Modelling Results

The geometry of the lake was modelled with an unstructured quadrilateral grid, allowing more flexibility for mapping a complex geometry compared to using a structured grid. Fig. 2 shows a projection of the grid seen from above. The lower figure of the central part of the lake shows the use of the unstructured grid to model the abrupt variation in the lake width.

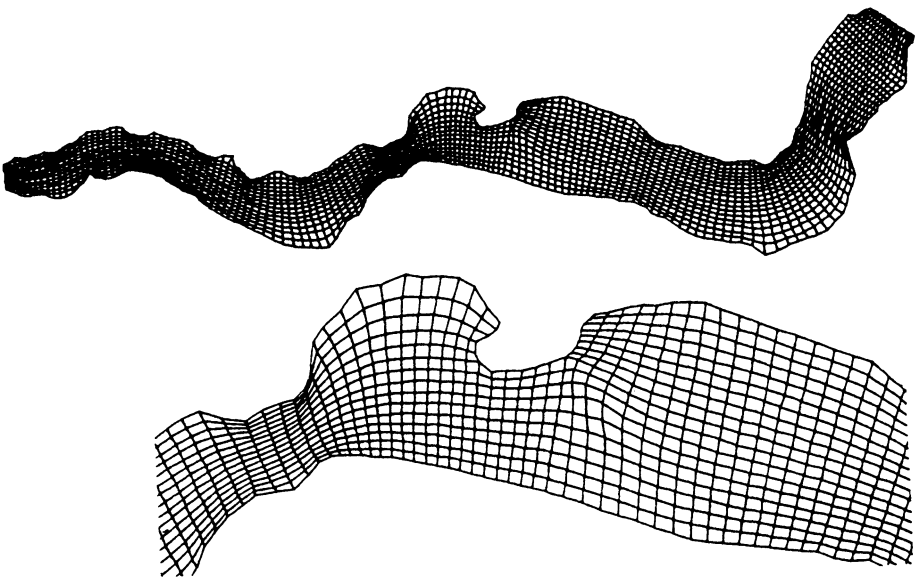

Fig. 2. Grid of lake Sperillen, seen from above. The upper figure is the whole grid and the lower figure is an enlargement of the central section.

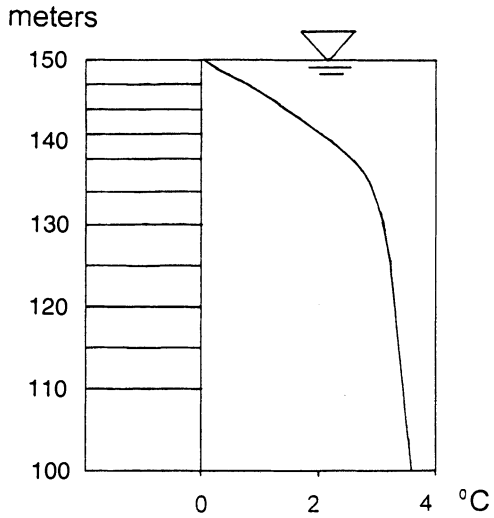

Fig. 3.
Vertical profile of temperature (right) and grid distribution (left).The vertical axis is metres above sea level.

The average measured temperature profile during January 1969, given in Fig. 3, was used to specify initial values at the start of the calculation. The water circulation was caused by an inflowing water discharge of 58 m^3/s with a temperature of 0.11°C. The temperature and discharge was fairly constant throughout the winter. At the location where the water entered the lake, the grid was relatively coarse. It was therefore not possible to model the complete mixing process in detail in this region. The inflowing water mixed with the warmer water below the ice, causing a temperature increase. A higher inflow temperature of 0.3°C was therefore used initially. This approximation will be discussed later.

Fig. 3 also shows the vertical grid distribution. The vertical grid size close to the water surface is 3 metres. The size increases towards the deeper parts of the lake, using a total of 12 cells. Field observations indicated that the current was confined to a layer 25 metres under the ice. The lake was therefore modelled with a constant depth of 50 metres. Most of the grid cells were located in the upper layer where the current was observed and where the vertical gradients were greatest.

The time step for the initial calculations was chosen to be 100 seconds. Using a much larger value caused instabilities. 15000 iterations were done, simulating a time period of 17 days.

The water entering the lake was colder than the lake water, also close to the ice cover. However, the field data showed that the temperatures close to the ice were higher in the current than elsewhere. It was assumed that this was because of turbulent mixing, as the current would move the warmer underlying water closer to the water surface. The ice thickness would thereby decrease over the current. It was therefore assumed that the modelling of the turbulence was important. The first calculations were carried out using the standard values for the damping term (Eq. (9)).

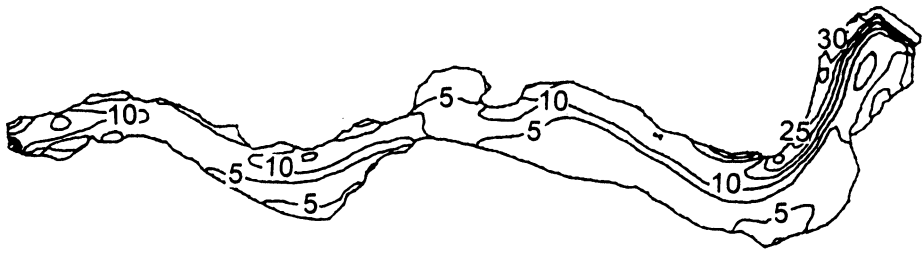

Fig. 4. Contour map of horizontal velocity close to the water surface. The values are given in mm/s.

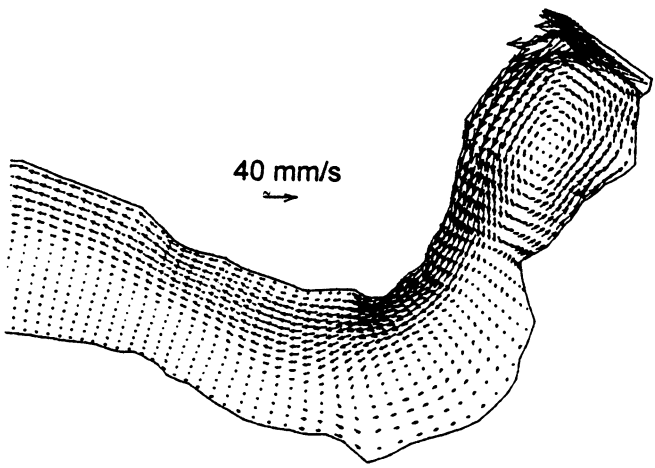

Fig. 5. Velocity vector map of the upstream part of the lake, close to the water surface.

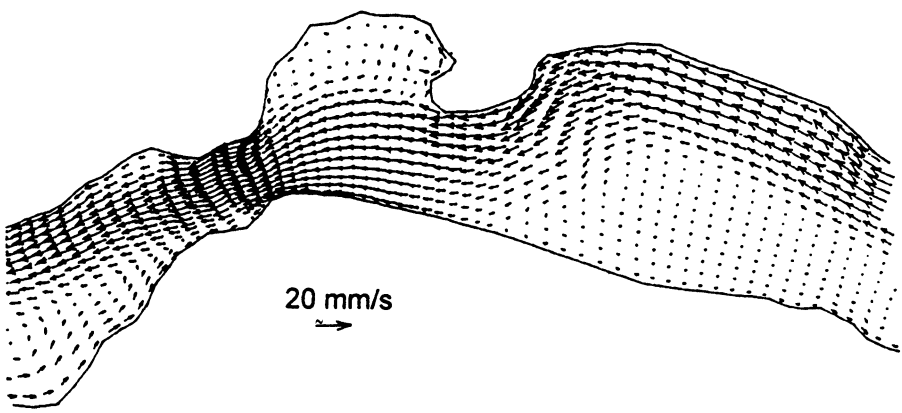

Fig. 6. Velocity vector map of the central part of the lake, close to the water surface.

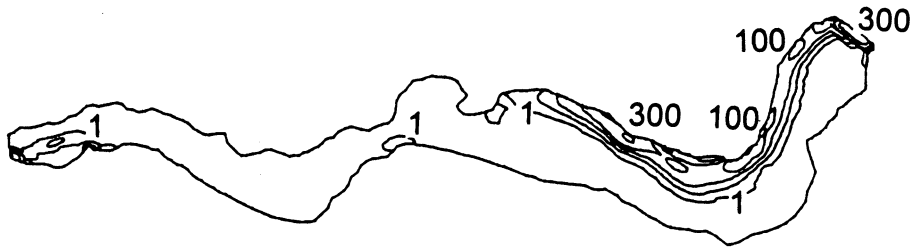

Fig. 7. Contour map of the eddy-viscosity at 7.5 meters depth. The values are given in mm^2/s.

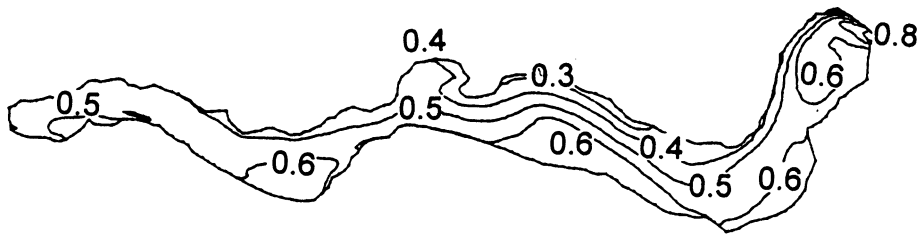

Fig. 8. Contour map of the vertical temperature gradient parameter, *S*, given by Eq. (1). The values are given in °C/m.

Initially, the default values of α and β was tested. This did not produce turbulence except at the water entrance. The *a* and *b* values were therefore modified. The value of β was set to 10 for all equations. Tests with an α value of –0.5 and –1.0 for all the equations gave too high eddy-viscosity, resulting in an incorrect current location. Using an α value of –1.3 gave better results. Fig. 4 shows a contour map of horizontal velocities close to the ice. Figs. 5 and 6 shows velocity vector maps at the same vertical location, but at the upstream and central part of the lake, respectively.

Comparing the results with the measured temperature gradient in Fig. 1, there is reasonably good agreement. A current is formed along the west bank of the lake, following the main geometry. The exception is the peninsula at the middle of the lake, where the radius of curvature is too small for the current to follow the bank. This also corresponds with the measurements and theoretical calculations (Tesaker 1973). Figs. 5 and 6 show a small return current on the east side, which was also observed in the field (Friis 1969). Comparing the measurements in Fig. 1 with Fig. 6, the current seems wider on the upstream side of the half-island. The reason could be the fairly coarse grid, which was not able to resolve the steep gradients.

Fig. 7 shows a map of the turbulent eddy-viscosity 7.5 metres below the ice. The values are higher in the current than elsewhere, indicating that the current will transport heat from the underlaying warm water to the surface. Theoretical evaluations of the field data (Friis 1969) also indicated this effect.

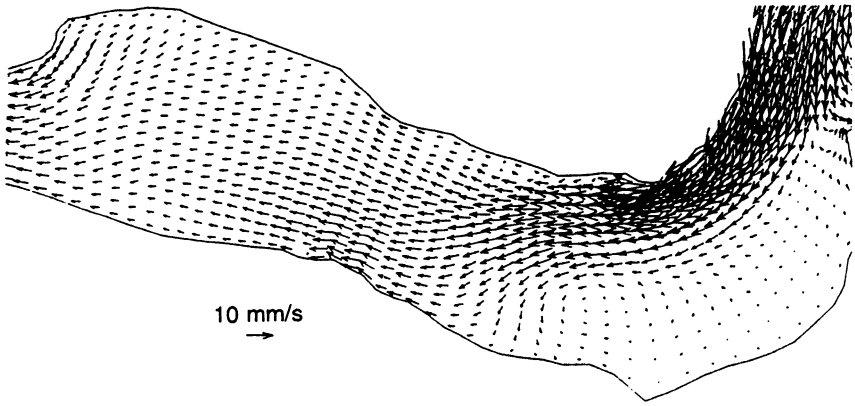

Fig. 9. Velocity vector map close to the water surface at the upstream part of the lake for a calculation without the Coriolis force.

In the original study based on the field data (Friis 1969), it was assumed that the current was located where the vertical temperature gradients were low. The temperature gradients were therefore also calculated in the numerical model, using the same formula (Eq. (1)). The result is shown in Fig. 8. The numerical model gave minimum values of the gradient parameter (Eq. (1)) at the west bank where the current was located, similar to the field observations (Friis 1969).

Some of the previous studies of the circulation in Sperillen (Friis 1969; Tesaker 1970) indicated the Coriolis force to be very important for the location of the current close to the west side of the lake. To investigate this further, a computation was done without the Coriolis force. The result is given in Fig. 9 with a velocity vector map close to the ice, at the upstream part of the lake. Comparing with Figs. 5 and 6, the current would not concentrate close to the west side of the lake, but spread out over the total width of the lake.

Parameter Sensitivity Test and Discussion

As described earlier, the measurements of Stigebrandt (1977) in Section A compared well with both Friis (1969) observations and the numerical model. In section B, however, Stigebrandt measured a more uniform velocity profile in the cross-streamwise direction. Comparing with the calculated velocities in Fig. 6, the numerical model corresponds better with Stigebrandt's results than with Friis for this section. It is difficult to say what is correct, as false diffusion may cause the more uniform profile in the numerical model. At the time Stigebrandt measured the velocities, the outflow of the lake was 20% more than the inflow. During Friis' measurements, this value was between 3 and 7%. In any case, the measurements can not be

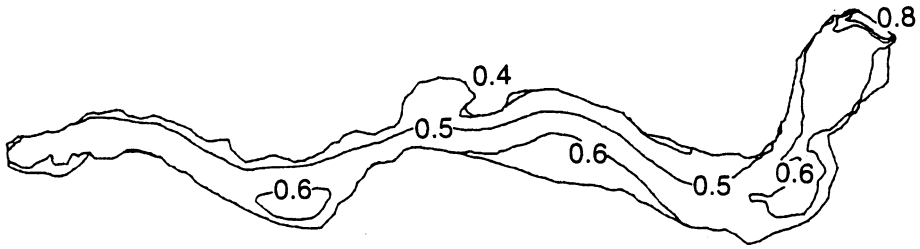

Fig. 10. Contour map of the vertical temperature gradient parameter, S, (Eq. 1) for the constant eddy-viscosity model. The values are given in °C/m.

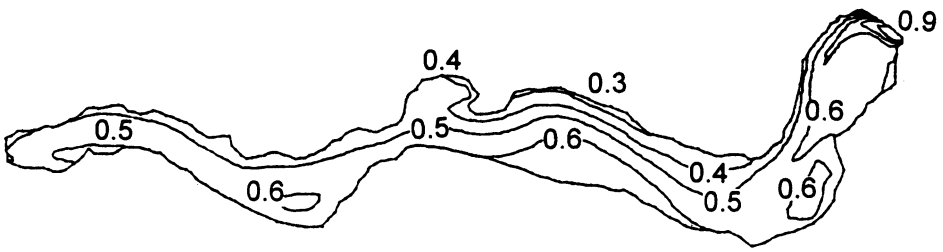

Fig. 11. Contour map of the vertical temperature gradient parameter, S, (Eq. (1)) for inflow temperature of 0.11 ^{0}C. The values are given in °C/m.

said to validate or invalidate the results from the numerical model for this cross-section.

A parameter sensitivity test was used to assess the effect of the uncertainty for some of the input parameters for the numerical model. An important process affecting the result was the turbulent mixing. A parameter study for the coefficients in Eq. (9) was described previously. To further assess the effect of the turbulence, the modified k-ε model was replaced by a constant eddy-viscosity model. Since the flow velocities were fairly small, around 2-3 cm/s, an effective viscosity equal to the kinematic viscosity of water was used. The results showed velocities and current location very similar to what was obtained using the modified k-ε model (Figs. 4-6). Fig. 10 shows the vertical temperature gradient parameter. Comparing with Fig. 8, the modified k-ε model gives a lower minimum value, corresponding better with the measured minimum values below 0.3°C/m.

Another topic in the parameter sensitivity test was mixing in the inlet zone and the input temperature. To assess the effect of the choice of 0.3°C, a calculation was run with an inlet temperature of 0.11°C. This gave the temperature gradient parameter map in Fig. 11, which can be compared with the standard calculation in Fig. 8. There is very little difference between the results, indicating that the result is not sensitive to this parameter.

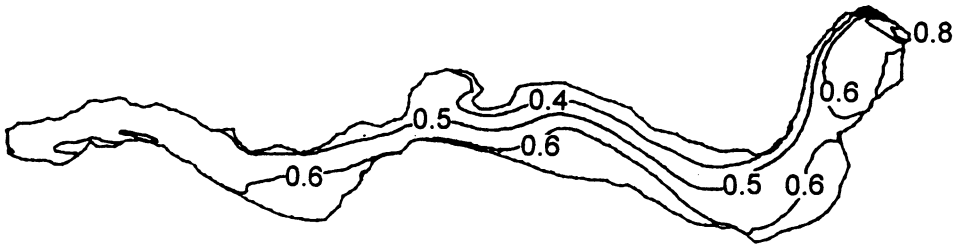

Fig. 12. Contour map of the vertical temperature gradient parameter, S, (Eq. (1)) for time step of 30 seconds instead of 100 seconds. The values are given in °C/m.

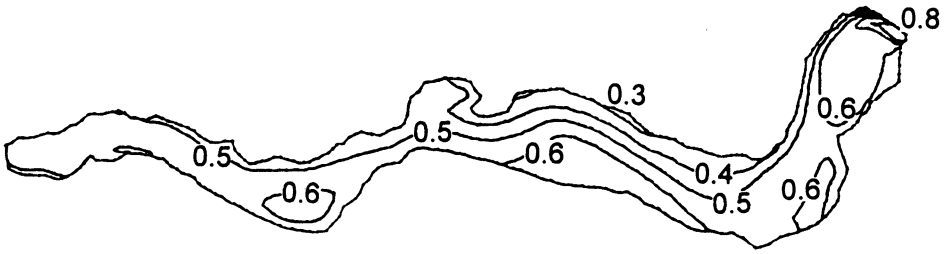

Fig. 13. Contour map of the vertical temperature gradient parameter, S, (Eq. (1)) for zero temperature flux across the ice. The values are given in °C/m.

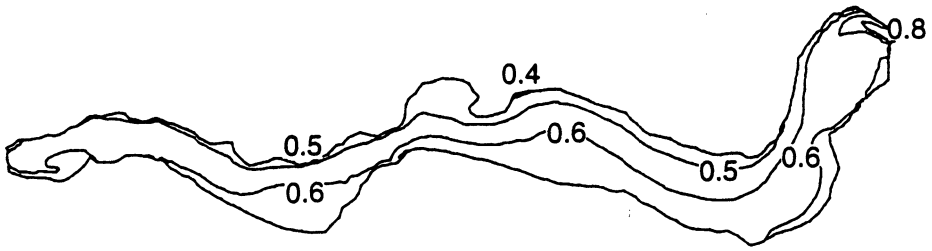

Fig. 14. Contour map of the vertical temperature gradient parameter, S, (Eq. (1)) using wall laws for turbulent flow at the ice. The values are given in °C/m.

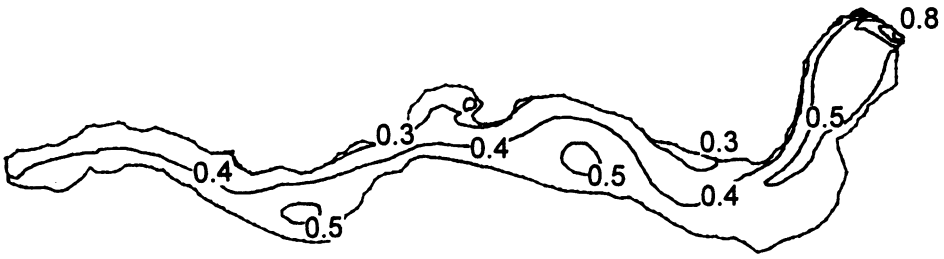

Fig. 15. Contour map of the vertical temperature gradient parameter, S, (Eq. (1)) after simulating 4 weeks instead of 2 weeks. The values are given in °C/m.

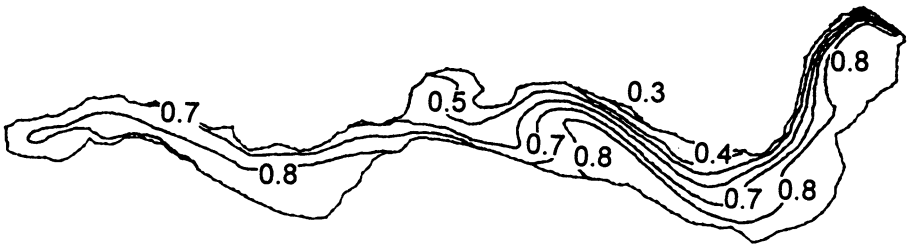

Fig. 16. Contour map of the vertical temperature gradient parameter, S, (Eq. (1)) for finer grid in the vertical direction and $\alpha = -1.4$ instead of -1.3. The values are given in °C/m.

The other parameters sensitivity tests included numerical parameters like the magnitude of the time step. Using a time step of 30 seconds instead of 100 seconds gave the temperature gradient parameter map in Fig. 12. Compared with Fig. 8, there is little difference between the results.

The effect of the heat flux across the water surface was investigated by setting it to zero. The resulting temperature gradient parameter map is given in Fig. 13. The result is fairly similar to the standard calculation in Fig. 8, although the cross-stream gradients are slightly lower. However, the result does not seem very sensitive to this parameter.

The other boundary condition at the ice was for the velocities. A no-slip boundary condition was used, being valid only for laminar flow. Eq. (9) reduced the eddy-viscosity close to the ice down to the value of the kinematic water viscosity for most of the lake. Only in a small area close to the entrance, the flow was turbulent. Using turbulent wall laws with 1 mm roughness in this region produced essentially the same flow pattern as without the wall laws. The temperature gradient parameter (Eq. (1)) gave a slightly smaller variation across the lake (Fig. 14).

To investigate the effect of the length of the simulation time, 34 days were simulated, twice the length of the previous calculations. The resulting temperature gradient parameter map is given in Fig. 15. The cross-streamwise gradients have decreased, but the overall gradient picture is the same. The decrease of the gradient may be caused by false diffusion over time. Since the POW scheme was used, false diffusion could be expected. The SOU scheme was therefore tested, to assess the effect of false diffusion. Unfortunately, this lead to instabilities, and the resulting water velocity field was not realistic or according to the field measurements. The reason was probably over and undershoots in the high-order scheme.

The other method to decrease false diffusion was to decrease the grid cell sizes. This was not possible in the horizontal directions due to limited computing resources. Instead, the number of grid cells in the vertical direction was increased from 12 to 23. The computational time increased to a week for one run. The time step had then been decreased to 50 seconds, to prevent instabilities. The first run

with the same turbulence damping coefficients as used previously gave too high diffusion, resulting in an incorrect current location. Modifying the parameter a from –1.3 to -1.4 gave a better result. The resulting temperature gradient parameter map is given in Fig. 16. Compared with the coarser grid results in Fig. 8, the cross-streamwise gradients are much steeper. As indicated at Fig. 16, the current also moved slightly away from the west side of the lake after the first right turn. The horizontal magnitude of the displacement was only about one kilometre, and the rest of the current was located in better correspondence with the observations.

It is likely that the high length/depth ratio of the grid cells could cause some of the instability problem in the current model. An interesting approach would be to decrease the grid cell sizes in the horizontal directions. This would probably also give a more exact location of the current. The problem would then be the very long computational times on the computers of today. However, since the cost of computational time presently is decreasing rapidly, this will be an interesting study in a few years from now.

Conclusions

The numerical model was able to predict the currents in the lake with reasonable agreement with the field measurements. The Coriolis force, together with the temperature stratification, formed a short-circuiting current at the west bank of the lake, leading to locally decreased ice thickness. Both a zero-equation model and the k-ε turbulence model gave reasonable result with respect to the water velocities. Using the k-ε model with a damping term, it was possible to model the turbulent mixing in the current, giving a better result for the temperature gradient.

The results using the modified k-ε model showed that it is possible to calculate the turbulent mixing in the current. However, the coefficients in Eq. (9) are based on calibration, and are therefore not general. It would be an advantage to derive a turbulence model with standard coefficients, like for example in the standard k-ε model. This would be a topic for further research.

Acknowledgements

We want to thank Mr. Jon Friis and the Begna River Water Management Group for the use of the measurements in Lake Sperillen and giving advice and additional data. We also would like to thank Dr. Einar Tesaker and Dr. Torkild Carstens at SINTEF for giving advice on the hydrodynamics of the lake. And we want to thank The Research Council of Norway for funding the numerical study.

Notations

δ_{ij} – Kronecker delta
ε – turbulent dissipation of k
ν – kinematic viscosity of water
ν_T – turbulent eddy viscosity
ρ – density of water
τ – shear stress
σ_k, σ_ε – constants in k-ε model
Γ – diffusion coefficient
c_μ – constant in k-ε model
k – turbulent kinetic energy
u – velocity
u_* – shear velocity
t – time
x – length scale
$c_{\varepsilon 1}$, $c_{\varepsilon 2}$ – constants in k-ε model
P – pressure
P_k – production of turbulent kinetic energy
U – velocity

References

Falconer, R. A., George, D. G., and Hall, P. (1991) Three-dimensional numerical modelling of wind driven circulation in a shallow homogenous lake, *Journal of Hydrology, Vol. 124*, pp. 59-79.

Friis, J. (1969) Temperatures in Lake Sperillen, Report no. 7/69, Department of Hydrology, The Norwegian Water and Electricity Authority (in Norwegian).

Gbah, M. B., Jacobs, S. J., Meadows, G. A., and Bratkovich, A. (1998) A model of the thermal bar circulation in a lone basin, *Journal of Geophysical Research – Oceans, Vol. 103*, No. C6, pp. 12807-12821.

Guting, P. M., and Hutter, K. (1998) Modeling wind-induced circulation in the homogenous Lake Constance using k-epsilon closure, *Aquatic Sciences, Vol. 60*, No. 3, pp. 266-277.

Huttula, T, Jopopnen, J., Lehtinin, K., Wahlgren, A., and Niinioja, R. (1996) Water currents and spreading of river load in Lake Pyhaselka, Saimaa, Finland, *Hydrobiologia, Vol. 322*, No. 1-3, pp. 117-124.

Malm, J. (1995) Spring circulation associated with the thermal bar in large temperate lakes, *Nordic Hydrology, Vol. 26*, pp. 331-358.

Olsen, N. R. B., Jimenez, O., Lovoll, A., and Abrahamsen, L. (1994) Calculation of water and sediment flow in hydropower reservoirs, 1st. International Conference on Modelling, Testing and Monitoring for Hydro Powerplants, Hungary.

Olsen, N. R. B. (1999a) Two-dimensional numerical modelling of flushing processes in water reservoirs, *IAHR Journal of Hydraulic Research, Vol. 37*, No. 1.

Olsen, N. R. B. (1999b) Computational Fluid Dynamics in Hydraulic and Sedimentation Engineering, Class notes, Department of Hydraulic and Environmental Engineering, The

Norwegian University of Science and Technology (can be downloaded from www.bygg.ntnu.no/~nilsol/cfd).

Tesaker, E. (1973) Horizontal cross-flow temperature gradient in a lake due to Coriolis' force, Int. Conference on Hydrology of Lakes, Helsinki, Finland.

Patankar, S. V. (1980) *Numerical Heat Transfer and Fluid Flow*, McGraw-Hill Book Company, New York.

Raja, R., Cetina, M., and Sirca, A. (1997) Hydrodynamic and water quality modelling: Case studies, *Ecological Modelling, Vol. 101*, No. 2-3, pp. 209-228.

Rodi, W. (1980) *Turbulence models and their application in hydraulics*, IAHR State-of- the-art paper.

Simons, T. J. (1974) Verification of numerical models of Lake Ontario: Part I, Circulation in spring and early summer, *Journal of Physical Oceanography*, Vol. 4, pp. 507-523.

Stigebrandt, A (1977) Hydrographic Measurements in Lake Sperillen 1975-1976 and in Lake Losna 1975, SINTEF Report No. STF60 A77024, Trondheim, Norway.

Received: 10 March, 1999
Revised: 29 June, 1999
Accepted: 11 October, 1999

Address:
Department of Hydraulic and,
Environmental Engineering,
Norwegian Univ. of Science and Technology,
N-7491 Trondheim, Norway.
Email: nils.r.olsen@bygg.ntnu.no